HHS Public Access

Author manuscript

Clin Cancer Res. Author manuscript; available in PMC 2017 February 01.

Published in final edited form as:

Clin Cancer Res. 2016 February 1; 22(3): 670–679. doi:10.1158/1078-0432.CCR-15-0190.

Targeting cancer stem cell in castration resistant prostate cancer

Eun-Jin Yun[1], **Jiancheng Zhou**[1,2], **Chun-Jung Lin**[1,3], **Elizabeth Hernandez**[1], **Ladan Fazli**[4], **Martin Gleave**[3], and **Jer-Tsong Hsieh**[1,5,*]

[1]Department of Urology, University of Texas Southwestern Medical Center, Dallas, TX 75390, USA

[2]Department of Urology, The First Affiliated Hospital, Medical School of Xi'an Jiaotong University, Xi'an 710049, China

[3]Graduate Institute of Clinical Medical Science, China Medical University, Taichung 40402, Taiwan

[4]VancouverProstate Center, University of British Columbia, Vancouver, British Columbia V6K 2P5, Canada

[5]Graduate Institute of Cancer Biology, China Medical University Hospital, Taichung 40447, Taiwan, Republic of China

Abstract

Purpose—Clinical evidence suggests an increased CSC in tumor mass may contribute to the failure of conventional therapies since CSCs seem to be more resistant than differentiated tumor cells. Thus, unveiling the mechanism regulating CSCs and candidate target molecules will provide new strategy to cure the patients.

Experimental design—The stem-like cell properties were determined by a prostasphere assay, and dye exclusion assay. To find critical stem cell marker and reveal regulation mechanism, basic biochemical and molecular biological methods such as qRT-PCR, Western blot, reporter gene assay and chromatin immunoprecipitation assay were employed. In addition, to determine the effect of combination therapy targeting both CSCs and its progeny, *in vitro* MTT assay and *in vivo* xenograft model was used.

Results—We demonstrate immortalized normal human prostate epithelial cells, appeared non-tumorigenic *in vivo*, become tumorigenic and acquire stem cell phenotype after knocking down a tumor suppressor gene. Also, those stem-like cells increase chemoresistance to conventional anti-cancer reagent. Mechanistically, we unveil that Wnt signaling is a key pathway regulating well-known stem cell marker CD44 by directly interacting to the promoter. Thus, by targeting CSCs using Wnt inhibitors synergistically enhances the efficacy of conventional drugs. Furthermore, the

*Correspondence: Jer-Tsong Hsieh, Ph.D., jt.hsieh@utsouthwestern.edu; Phone: 214-648-3988; Fax: 214-648-8786; 5323 Harry Hines, J8-134 Dallas, TX 75390, USA..

All the authors except Dr. Gleave is a founder of OncoGenex, do not have any conflict of interest.

in vivo mice model bearing xenografts showed a robust inhibition of tumor growth after combination therapy.

Conclusions—Overall, this study provides strong evidence of CSC in CRPC. This new combination therapy strategy targeting CSC could significantly enhance therapeutic efficacy of current chemotherapy regimen only targeting non-CSC cells.

Keywords

DAB2IP; CD44; Cancer Stem Cell; Wnt pathway

Introduction

Cancer stem cells (CSCs) share many characteristics with somatic stem cells, such as immortality and self-renewal. In addition to normal stem cell properties, CSCs appear to be tumor initiators and show resistance to therapies because of their quiescence. Increasing evidence indicates that CSCs are present in the end stage of disease (1). Although the cell origin of CRPC remains controversial, several studies clearly indicate the presence of CSC in CRPC (2, 3). Despite of many potential stem cell markers identified in prostate, in human PCa, the $CD44^+/CD24^-$ cells have been associated with the prostate cancer stem cell (PCSC) (4). CD44 has been implicated in numerous biological processes including cell adhesion, migration, drug resistance and apoptosis (5-7). Furthermore, many studies implicate CD44 in PCa development and invasion *in vitro* as well as in metastatic dissemination *in vivo* (8, 9). However, the mechanism(s) associated with elevated CD44 in PCa is largely unknown.

DAB2IP is characterized as a novel tumor suppressor in PCa metastases by inhibiting epithelialto-mesenchymal transition (EMT) (10, 11). Besides, our recent study showed that DAB2IP had a critical role in suppressing stemness through modulating CD117 transcription (12). In this study, we demonstrate that loss of DAB2IP (10, 13) expression in non-tumorigenic normal prostate epithelia derived from androgen receptor-negative basal cell population also increases their tumorigenicity, stemness and chemo-resistance. Unlike PCa cell lines which were used in previous study (12), these normal prostate epithelial cell populations exhibit $CD44^+/CD24^-$ instead of $CD117^+$ suggesting existence of another regulation mechanism. Apparently, CD44 is not only a stem cell marker correlated with PCa progression but also a driver for PCSC formation in which Wnt pathway is further identified as a key underlying mechanism in modulating CD44 expression. Based on these findings, we developed a combination strategy using Wnt inhibitor and docetaxel to target both CSC and its progeny non-CSCs respectively, to significantly enhance therapeutic efficacy of CRPC. Overall, this study provides strong evidence of CSC in CRPC and offers a new therapeutic regimen for CRPC.

Materials and Methods

Cell culture and reagents

PZ-HPV7 and RWPE-1 are immortalized human prostate epithelial cell line by human papillomavirus 18; PZ-HPV7 was obtained from Dr. Peehl (Stanford Univ.) (14) and

maintained in PrEGM media (Lonza). RWPE-1 was obtained from Dr. Yen (Univ. of Rochester) (15) and maintained in Keratinocyte media (Lifetechnologies) supplemented with 10% FBS and penicillin/streptomycin. PZ-HPV7T established as described previously (13), Du145 and 22Rv$_1$ (ATCC) cells were grown RPMI1640 (Lifetechnologies) supplemented with 10% FBS and penicillin/streptomycin. All cells were mycoplasma-free and maintained at 37ºC with 5% CO_2 in a humidified incubator. Cell lines were authenticated using AmpFLSTR®Identifier® PCR Amplification kit (Applied Biosystems, Grand Island, NY) every 6 months.

Wnt inhibitor IWP-2 and LGK974 were purchased from Calbiochem and Xcessbio Biosciences Inc., respectively. CD44S pWZL-Blast was a gift from Robert Weinberg (Addgene plasmid #19126).

Colony assay

Cells were collected after trypsinization, and re-suspended in the complete media. Single cell suspensions were plated in 6-well plate at the clonal density of 1,000 cells per dish. After 10 days of culture, colonies were fixed with 4% paraformaldehyde for 10 min, stained with crystal violet for additional 10 min, and washed with 1X PBS. The colonies were photographed. The colony numbers were counted using Image J analysis software. Particle Analysis program was used for counting the colony numbers.

Anchorage independent growth assay

To make the bottom layer, 1 ml of 0.6% agarose was added to 6-well plates, and allowed to gel at room temperature. To prepare the top layer (0.3% agarose), 500 µl of agarose was mixed with 500 µl cell suspension containing the 10,000 cells. This mixture were overlaid above the bottom layer and allowed to solidify at room temperature. An additional 2 ml of culture media was added after solidification to the top layer, and cells were incubated for 2 weeks at 37°C. After 14 days of growth, the colonies were photographed. The colony numbers were counted under a phase contrast microscope. Data was presented as colony numbers per field.

In Vitro invasion and migration assay

In vitro invasion was determined in the Matrigel-based assay. Briefly, 6.5 µm polycarbonate filters of Transwell (24-well insert; pore size = 8 µm; Corning) were coated with 25 µg Matrigel. The lower chambers of Transwell were filled with 600 µl of serum-free medium and the cells were plated in the upper chamber (5×10^4 cells/200 µl/chamber). After incubation for 48 h, non-invading cells on the upper surface of the membrane were removed by a cotton swab and cells on the lower surface were stained with crystal violet and quantified by measuring OD_{560nm} with 96-well plate. The cell migration assay was performed with the same method except for Matrigel-coated membrane.

Prostatasphere assay

Prostate sphere growth was based on Lawson et al. (16). 3×10^3 Cells in PrEGM media were mixed 1:1 (v/v) with Matrigel (BD Bioscience Cat.No.354234, 9-12 mg/ml) in a total volume of 300 µl. Each sample were subsequently plated into 24-well plate and allowed to

solidify for 15 min, after which 1 ml PrEGM media was added. Cells were thereafter replenished every 3 days, by the removal of 0.5 ml of spent media and the addition of 0.5 ml of fresh media. Spheres were counted 14 days after plating.

Hoechst 33342 dye exclusion assay

The protocol was based on Kim *et al.* (17) with slight modifications. Briefly, cells (1×10^6 cells/mL) were seeded in 10-cm culture dishes allowed to attach and washed two times with PBS. Then, the cells were incubated with Hoechst 33342 (5 μg/mL, Lifetechnologies) in medium containing 5% FBS at 37°C for 90 min. After washing with PBS, cells were swiftly trypsinized and washed with ice cold PBS. Cells were then filtered and re-suspended in ice cold PBS. Propidium iodide (5 μg/mL) was added 5 min before analysis to discard dead and apoptotic cells. Cells were analyzed by DakoCytomation MoFlo cytometer using dual-wavelength analysis (blue, 450/20 nm; red, 670 nm) after excitation with 350 nm UV light.

Quantitative real-time PCR (qRT-PCR)

Total RNA was extracted with RNeasy mini kit (QIAGEN) and 1 μg RNA was reverse transcribed with Vilo cDNA synthesis kit (Lifetechnologies). Real-time PCR analysis was set up with SYBR Green Supermix kit (Lifetechnologies) and carried out in MyiQ thermal cycler (Bio-Rad). The relative level of target mRNA was determined by normalizing 18S rRNA. All experiments were repeated at least twice to triplicate results.

Flow cytometry and fluorescence-activated cell sorting

For detection of cell surface expression of CD24 and CD44, cells were incubated with APC-conjugated human monoclonal CD24 Ab (BD Biosciences) and PE-conjugated human monoclonal CD44 Ab (BD Biosciences) for 30 min, and analyzed using flow cytometry (FACS Calibur, BD Biosciences). Cell sorting was performed with FACSAria cell sorters (BD Biosciences).

Transfection and luciferase reporter assay

Cells were seeded in 24-well plate with 70% confluency before transfection. Cells were co-transfected with luciferase reporter plasmids (0.5 μg/well) and internal control, pRL-TK (Promega; 2 ng/well), expressing the *Renilla* luciferase. Transfections were performed using Xfect (Clontech) according to the manufacturer's instructions. 48 h after transfection, the wells were rinsed twice with phosphate-buffered saline, and cells were harvested with 200 μl of passive lysis buffer (Promega). Following a brief freeze-thaw cycle, the insoluble debris was removed by centrifugation at 4°C for 2 min at 14,000 rpm. Aliquots of the supernatant (20 μl) were then immediately processed for sequential quantitation of both firefly and *Renilla* luciferase activity (Dual-Luciferase Assay System, Promega) using a Monolight TD 20/20 luminometer (Turner Designs). The activity of the *Renilla* reporter plasmid was used for normalization of transfection efficiency. All transfection experiments were performed in triplicates.

Western blot

Cells were washed twice with PBS and lysed in ice-cold lysis buffer [150 mM NaCl, 1% Triton X-100, 0.5% sodium deoxycholate, 0.1% SDS, 50 mM Tri (pH 8.0), protease inhibitor cocktail (Roche)], and cleared by microcentrifugation. Equal amounts of protein were subjected to electrophoresis on 7% or 10% NuPAGE gels (Lifetechnologies). Separated proteins were transferred onto nitrocellulose membranes, and membranes were incubated with 2% nonfat dry milk (w/v) for 1 h and then washed in PBS containing 0.1% Tween 20. Membranes were then incubated with primary antibody (Ab), and Ab binding was detected using the appropriate secondary Ab coupled with horseradish peroxidase. Primary Abs used were as follows: mouse monoclonal anti-Actin was purchased from Sigma, mouse polyclonal anti-GSK3β was from Santa Cruz Biotechnology, rabbit polyclonal anti-β-catenin, phospho-β-catenin (T41/S45) and phospho-GSK3β (S9) were from Cell Signaling.

Chromatin-immunoprecipitation assay (ChIP assay)

ChIP assay were performed by using ChIP-IT Express Enzymatic kit (Active motif, Cat#53009) according to the manufacturer's instructions. In briefly, cells were cross-linked with 1% formaldehyde for 10 min, quenched with glycine followed by nuclear lysis. After isolating nuclear fractions, chromatin was enzymatically sheared into 200-100 bp. The sheared DNA was immunoprecipitated with ChIP-grade Ab for 16 h. After reversal of cross-linking, DNA fragments were purified on spin columns (Active motif, Cat#58002). The β-catenin binding site in the CD44 promoter was amplified by PCR from purified chromatin. The primers used in this experiment were listed in Table S2.

In vitro cytotoxicity assay

Cells (5×10^3) were seeded in 96-well plates. After 24 h, media were changed with serum-free media for 4 h and then different concentrations of drugs treated for 48 h. In vitro cytotoxicity was measured using 3-(4,5-dimethylthiazol-2-yl)-2,5-diphenyltetrazolium bromide (MTT) assays according to the manufacturer's instructions (Roche). Drug synergistic effects were determined based on combination index (CI) (18).

Mouse xenografts

All animal work was approved by the Institutional Animal Care and Use Committee. Du145 (1×10^6 cells/site) cells were subcutaneously injected into six-week-old male SCID mice. When tumors developed as measurable size, drug treatment started and tumor volume (cubic millimeters) was measured. Treatment schedules were docetaxel (5 mg/kg/i.p.), LGK974 (2 mg/kg/oral gavage) and combination of them twice a week for 3 weeks. Tumor volume was calculated by using the ellipsoid formula ($\pi/6 \times \text{length} \times \text{width} \times \text{depth}$).

Clinical specimens, IHC and scoring system

This study was done on the total of 194 PCa specimens obtained from Vancouver Prostate Centre Tissue Bank. 76 of those cases were subjected to neoadjuvant hormone therapy (NHT). The H&E slides were reviewed and the desired areas were marked. Three TMAs were manually constructed (Beecher Instruments, MD, USA) by punching duplicate cores of

1 mm for each sample. All the specimens were from radical prostectomy. Tissue samples were arrayed according to Gleason score, primary or CRPC status, and with or without NHT, respectively. The Institutional Review Board of UT Southwestern and Vancouver General Hospital, BC Canada approved the tissue procurement protocol for this study, and appropriate informed consent was obtained from all patients.

Specimens were stained with Abs specific for CD44 (Company, 1:200) and DAB2IP (1:400) using Ventana autostainer model Discover XT ™ (Ventana Medical System, Tuscan, AZ). The expression of DAB2IP or CD44 was scored based on percentage and intensity according to Allred's scoring protocol (19). Values on a four-point scale were assigned to each specimen. The intensity score was assigned, which represented the average intensity of positive cells (0, none; 1, weak or questionably present stain; 2, intermediate intensity in a minority of cells; and 3, strong intensity in a majority of cells). All slides were scored independently by two investigators who were blinded to patient clinical information.

Statistical analysis

All error bars in graphical data represent mean ± SD. Student's two-tailed t-test was used for the determination of statistical relevance between groups, and $p<0.01$ was considered statistically significant. All statistical analyses were performed with GraphPad Prism software.

Results

Loss of DAB2IP transforms normal prostate epithelia into CSC

Previous studies have demonstrated that loss of DAB2IP expression elicit EMT which have been associated with CSC development (11, 20). To determine whether loss of DAB2IP is capable of transforming non-tumorigenic normal prostate epithelia derived from androgen receptor-negative basal cell population, two well-characterized cell lines (21) were employed. The clonogenic ability was significantly increased in both RWPE-1 knock down (KD) and PZ-HPV7 KD cells (Fig. S1A). Data from soft agar assay showed a significant increase in anchorage independent growth of KD cells (Fig.S1B) and PZ-HPV7 KD cells became tumorigenic *in vivo* (10).

Noticeably, both KD cells increased stemness properties. For example, RWPE-1 KD or PZ-HPV7 KD cells were able to form spheroid prostaspheres (Fig.S1C) but the majority of Con cells failed to form measurable prostatspheres in semisolid culture for 2 weeks. These KD cells exhibited significant sphere-forming ability in both numbers (Fig.S1C, left panel) and size (Fig.S1C, right panel). In addition, the side population (SP) associated with drug efflux capacity measured by Hoechst 33342 dye exclusion is commonly used for characterizing hematopoietic stem cell and CSCs (22). As shown Fig.S1D, the percentage of SP increased significantly in both RWPE-1 KD and PZ-HPV7 KD cells. In addition, loss of DAB2IP significantly increased *in vitro* migration and invasion (Fig.S2A, B). Together, these results suggest that KD cells have acquired stem cell phenotypes.

PCSC cells exhibit enriched CD44$^+$/CD24$^-$ populations

To identify specific stem cell markers associated with these KD cells, we screen several stem cell markers and the results showed the consistent elevation of CD44 mRNA expression and reduction of CD24 mRNA expression in both RWPE-1 and PZ-HPV7 KD cell (Fig.1A, Fig.S3A and B) while the expression pattern of other CSCs surface markers was vary. Flow cytometric analysis (Fig.1B) also demonstrated that the CD44$^+$/CD24$^-$ populations were significantly higher in both KD cells whereas most Con cells exhibit CD44$^-$/CD24$^+$ expression suggesting that DAB2IP is a potent suppressor for stemness phenotype acquisition. To find the driving force of CSCs, we more focused on elevated CD44 rather than depleted CD24, and interestingly, PZ-HPV7T cells (13), a tumorigenic subline of PZ-HPV7 showed elevated CD44 expression as well as sphere forming ability compared to wild-type cells (Fig.S3C). By sorting PZ-HPV7T cells into CD44$^+$ and CD44$^-$ population, CD44$^+$ cells exhibit significantly lower DAB2IP mRNA (Fig.1C, left panel) and protein (Fig. 1C, right panel) than CD44$^-$ cells or parental cells. Consistently, lymph node metastatic PCa tissues exhibited a strong CD44 staining on cell membrane inversely correlated with DAB2IP expression (Fig.1D, left panel, Fig. S3D). A significant difference was detected between primary and metastatic tissues for DAB2IP and CD44 respectively (Fig.1D, right panel). In addition, we also noticed that CD44 mRNA expression was elevated in DAB2IP knock-out (KO) mice compared with wild-type mice tissue (Fig.S3E); prostate epithelia from DAB2IP KO mice exhibited hyperplasia in castrated host (11). Taken together, DAB2IP is a potent regulator in modulating CD44 gene expression enriched in PCSC.

Wnt signal pathway mediate the regulation of CD44 by DAB2IP

Mechanistically, the presence of DAB2IP was able to inhibit CD44 gene transcription (Fig. S4A) that CD44 gene promoter activity increased in both KD cells compared to their Con cells respectively. To reveal the possible mechanism of DAB2IP in regulating CD44 transcription, the structural-functional relationship of DAB2IP that contains several unique domains with distinct functional role (11) was carried out. As shown in Fig.2A, the C2 domain of DAB2IP is the key domain in suppressing CD44 gene promoter activity. It is known that C2 domain in DAB2IP can recruit PP2A to activate GSK3β that is able to inhibit β-catenin/Wnt signaling (11). Indeed, in both RWPE-1 and PZ-HPV7 KD cells, activities of β-catenin and the downstream gene were activated by measuring Wnt-specific gene reporter activity (i.e., TOP) (Fig.2B, left panel and Fig.2C). Consistently, PZ-HPV7T cells with elevated CD44 and CD44$^+$ population sorted from both PZ-HPV7T and Du145 cells (Fig. 2B, right panel). Furthermore, analyses of several PCa clinical data demonstrated a positive correlation between β-catenin and CD44 expression (Fig.S4B, C and D). The data supports the role of β-catenin/Wnt signaling in regulating CD44 gene transcription. However, treatment of AR inhibitor could not change the CD44 expression in both cell lines suggesting CD44 was regulated in AR-independent pathway (Fig.S5). Besides, the effect of DAB2IP did not limited to specific CD44 isoforms but all isoforms' expression responded in a same pattern (Fig.S6). To further confirm the the regulation mechanism through Wnt pathway, the effect of Wnt inhibitors such as LGK974 and IWP-2 on CD44 expression in KD cells were examined. As shown in Figure 2D, the relative transcriptional activities of CD44 in KD cells significantly decreased by the treatment of both inhibitors. Treatment of

Wnt inhibitors also decreased both sphere formation (Fig. S7A) and expression of CD44 in KD cells (Fig. S7B). In contrast, the expression of constitutively active (CA) β-catenin mutant (S37A) in Con cells increased CD44 gene promoter activity (Fig.S8A) as well as *in vitro* cell migration and invasion in presence of DAB2IP (Fig.S8B and C). In KD cells, by reconstituting PP2A-WT or GSK3β (WT or CA) with DAB2IP could suppress CD44 gene promoter activity but PP2A-LP (catalytic inactive) failed to have the same effect (Fig.S8D). Also, the treatment of PP2A inhibitor Okadaic acid (OA) increased CD44 gene promoter activity in a dose dependent manner (Fig.S8E). To demonstrate the direct interaction between β-catenin and CD44 gene promoter region, ChIP data (Fig.3A) clearly showed that the direct binding of β-catenin to several CD44 gene promoter regions, based on the predicted β-catenin binding consensus sequences, in PZ-HPV7 KD cells. Also, ectopic expression of CA β-catenin in both PZ-HPV7 Con and 293 cells increased its binding to CD44 gene promoter (Fig.3A, B and C) and enhanced CD44 expression in RWPE-1 and PZ-HPV7 Con cells (Fig.3D). Taken together, these results conclude the direct effect of Wnt-elicited-β-catenin on CD44 gene expression in PCSCs.

CD44 drives PCSC associated with chemo-resistance

Despite CD44 is known as a stem cell marker, it is also a receptor for hyaluronic acid and can also interact with other ligands, such as osteopontin, collagens, and matrix metalloproteinases (5). Thus, to determine whether CD44 is a key driver for PCSC associated with chemo-resistance, CD44 expression was knock-downed using shRNA. Data (Fig.4A) indicated that CD44 KD significantly decreased *in vitro* tumorigenicity and sphere formation in PC-3 and $22Rv_1$ cells (Fig.4B and C). Also, decreased CD44 expression could sensitize these cells to docetaxel treatment (Fig.4D). All together, these data support the potency of CD44 in facilitating the onset of PCSC and increasing its chemo-resistance.

CRPC therapy targets CSC and its progeny

Docetaxel is the first line of chemotherapy for the CRPC patients who had unsuccessful androgen deprivation therapy (23). Nevertheless, CRPC develops to its resistant status very rapidly; it is believed that docetaxel can only kill proliferative progeny cells derived from CSCs, but fails to eradicate CSC (24). As shown in Fig. 5A, enriched CSC of RWPE-1 KD or PZ-HPV7 KD cells showed significant resistance compared with their Con cells treated with docetaxel. Nevertheless, RWPE-1 KD and PZ-HPV7 KD cells were slightly more sensitive to LGK974 than their Con cells (Fig. 5A, right panel). Similarly, $CD44^+$ cells sorted from PZ-HPV7T showed higher resistance to docetaxel but more sensitivity to LGK974 than $CD44^-$ cells (Fig.S9A). These results prompt us to explore a new therapeutic strategy by combining Wnt inhibitor with docetaxel to target CSC and its progeny cells. Indeed, RWPE-1 KD and PZ-HPV7 KD cells treated with combination regimen exhibited a synergistic effect (Fig.5B). As expected, CD44 mRNA expression level was decreased in these KD cells treated with LGK974 alone or combination, but not docetaxel alone (Fig.5C). Consistently, LGK974 alone or combination treatment significantly decreased the prostasphere formation of KD cells, but docetaxel failed to have any effect (Fig.5D). Similar results were observed from IWP-2 alone or in combination with docetaxel treatment (Fig.S9B and C). Furthermore, this combination therapy showed synergistic effect on PZ-HPV7T cells (Fig.S9D) as well as $22Rv_1$ cells (Fig.S9E) with the similar pattern of

decreasing $CD44^+$ cell population (Fig.S9F). On the other hand, constitutive overexpression of CD44S (25) in RWPE-1 and PZ-HPV7 KD cells, could overcome the effect of Wnt inhibitors and show increased cell viability (Fig.S10). These results support the hypothesis that to eradicate cancer completely, we must simultaneously target cancer-initiating cells and their progeny cell.

We further evaluate the *in vivo* effect of this combination strategy using CRPC model of Du145 cells which exhibit high percentage of $CD44^+$ population. The effect of combination treatment on Du145 cell line was determined *in vitro* and result showed the consistent results with KD cells (Fig.S11). Then, the mice bearing DU145 tumors were treated with docetaxel alone, LGK974, or combination of docetaxel with LGK974. Remarkably, mice treated with the combination treatment targeting both $CD44^+$ population and their progeny $CD44^-$ fast growing cells showed a robust inhibition of tumor growth compared with mice treated with single agent (Fig.6A and B). We noticed decreased CD44 and β-catenin levels in tumors harvested from LGK974 or combination treatment, whereas docetaxel treatment led to an increased CD44 expression, which further validated the outcome of targeted therapy (Fig.6C and D). Taken together, Wnt inhibitor can suppress CSC population and synergize the effect of conventional therapeutics on eradicating proliferative CSC progeny in CRPC.

Discussion

Human primary PCa is a typical androgen-dependent (AD) disease and most of tumor cells express differentiated luminal cell markers such as CK8 and 18, but are absent of basal cell markers (26). Androgen deprivation therapy (ADT) is the gold standard regimen for metastatic PCa patients. Despite the initial response, most patients eventually relapse and progress to CRPC, chemotherapy is the only option for these patients. However, only half of the patients respond to chemotherapy and even those who initially respond to treatment eventually become resistant (26). It appears that CRPC exhibits many similar phenotypes of stem cell (27), suggesting that clonal expansion of PCSC population and/or de-differentiation of PCa cells. It is believed that CSCs share many similar characteristics with normal stem cell; however they acquire additional malignant properties, such as uncontrolled division of progeny cell, invasion/metastasis, and chemo-resistance, which eventually lead to the mortality of cancer patients (28). New therapeutic regimens have greatly improved the survival of PCa patients, however the relapse of chemo-resistant tumor remains the major obstacle of complete cure of PCa (29). In general, most therapeutic regimens only target the proliferative tumor cells, as the progeny cell from quiescent CSC population still remaining intact. Consequently, the expansion of CSC population results in drug resistance (30). Understanding the underlying mechanisms associated with CSC and chemo-resistance could lead to new strategies for targeting CSC.

Loss of DAB2IP is frequently detected in high-grade and metastatic PCa tissues and correlated with biochemical-recurrence free survival of PCa patients (11, 31). Recent data (11) indicate that DAB2IP is able to intervene EMT as an initial step of PCa metastasis. EMT is associated with embryo implantation, embryogenesis, and organ development; however, it symbolizes de-differentiation of differentiated neoplastic cells. Apparently, loss

of DAB2IP in prostate epithelia also enhances PCSC phenotypes associated with enriched $CD44^+$ cell population. CD44 is a receptor for hyaluronic acid and commonly expressed in embryonic, hematopoietic, mesenchymal stem cells (32, 33). In PCa cells, CD44 has been implicated as a CSC marker and enriched $CD44^+$ cells were more tumorigenic and metastatic than $CD44^-$ cells (33). Elevated CD44 in PCa has been also implicated in cancer cell proliferation, tumorigenicity, migration, invasion and metastasis (34). We provide further evidence for the functional role of CD44 in maintaining CSC phenotype and the underlying mechanism of DAB2IP as a potent modulator for CD44 gene expression that is also supported by clinical data. CD44 comprises two kinds of exons, constant and variable ones. Former encode the extracellular globular part (exon 1-5), a short stem as connection to the cell membrane (exon 16 and 17) and the transmembrane domain (exon 18). Exon 19 and 20 are subject to alternative splicing creating either a short or more often a long cytoplasmic tail (35). The exons 6-15 are variable (v1-10), enlarging the stem on its distal site and forming several distinct CD44 isoforms, referred to as CD44 variants (CD44v1-10) (35). However, whether CD44s or CD44 variants is a critical CSCs marker is still under debate. Lacking all variable exons, CD44 standard (CD44s) is the most ubiquitous isoforms, and the expression pattern of the different variants of CD44 varies during lineage commitment. For example, epithelial cells express CD44v8 and CD44v6 is upregulated in monopoiesis and downregulated in granulopoiesis (36). Besides, CD44v6 is found to confer metastatic behavior to non-metastatic tumor cells, so associated with prostate cancer metastasis and chemo-/radioresistance (37, 38). In this study, we also made an effort to find the key driver which was involved in CSCs regulation, but DAB2IP equally regulated CD44 variants with loss of DAB2IP altered all types of CD44 variants including CD44v3, CD44v6 and CD44v8.

The mechanism(s) regulating CD44 gene expression in PCa cells is largely undefined (6, 39-41). In other cancer types, transcriptional factors such as Egr-1 and AP-1 are known to regulate CD44 expression (42, 43). However, we could not validate in PCa cells (data not shown). Here, we demonstrate a new mechanism of CD44 gene regulation by Wnt in which a direct binding of β-catenin-TCF/LEF complex to its gene promoter in PCa. Wnt signaling has been implicated in regulating stem cells from a variety of tissues (44, 45) and its dysregulation is associated with various cancers (46). Several studies indicated that an increased nuclear β-catenin is often detected in advanced stage of PCa (47) and $CD44^+$ cells are found to predominate in visceral metastases (9). Also, a recent study indicated that the interaction between PCa and bone which resulted in the resistance to androgen deprivation is mediated by bone stroma-derived Wnt5A (48). Collectively, $CD44^+$ in PCa cells may be responsible for chemo-resistant CRPC, thus, targeting Wnt appears be a viable therapeutic option in CRPC patients.

It is known that CSCs are more resistant to therapies because of the inherited survival advantage of CSC from increased anti-apoptotic or/and drug efflux machinery (49). Emerging studies indicate the onset of CSC associates with lethal phenotypes of many types of cancer. Thus, identifying therapeutic target to eradicate CSC becomes an urgent task to improve therapeutic outcome. Although Wnt inhibitors are able to decrease $CD44^+$ population, they fail to achieve significant therapeutic efficacy because the tumor mass population majority are proliferative CSC progeny cells. Conventional drug such as

docetaxel could target this population, thus combining both agents is likely to generate a more potent effect; indeed our data offers a new therapeutic strategy that combination of CSC and non-CSC targeting agents produce a synergistic anticancer efficacy.

Together with our recent report (12), DAB2IP is a critical modulator in the differentiation of PCa cells; loss of DAB2IP in PCa could elicit de-differentiation of PCa cells towards stemness phenotypes. Most encouragingly, the outcome of this experimental therapeutic model provides the immediate clinical translation of a potential targeted therapy for CRPC patients because this oral-bioavailable LGK974 with a wide-spectrum inhibition of Wnt pathway is under clinical trials for cancer (50).

Supplementary Material

Refer to Web version on PubMed Central for supplementary material.

Acknowledgement

We thank Mr. John Santoyo for editing this manuscript.

Grant Support

This work was supported in part by grants from the United States Army (W81XWH-11-1-0491 to JTH) and National Institutes of Health (CA182670 to JTH).

References

1. Li F, Tiede B, Massague J, Kang Y. Beyond tumorigenesis: cancer stem cells in metastasis. Cell Res. 2007; 17:3–14. [PubMed: 17179981]
2. Qin J, Liu X, Laffin B, Chen X, Choy G, Jeter CR, et al. The PSA(-/lo) prostate cancer cell population harbors self-renewing long-term tumor-propagating cells that resist castration. Cell stem cell. 2012; 10:556–69. [PubMed: 22560078]
3. Vander Griend DJ, Karthaus WL, Dalrymple S, Meeker A, DeMarzo AM, Isaacs JT. The role of CD133 in normal human prostate stem cells and malignant cancer-initiating cells. Cancer Res. 2008; 68:9703–11. [PubMed: 19047148]
4. Hurt EM, Kawasaki BT, Klarmann GJ, Thomas SB, Farrar WL. CD44+ CD24(-) prostate cells are early cancer progenitor/stem cells that provide a model for patients with poor prognosis. Br J Cancer. 2008; 98:756–65. [PubMed: 18268494]
5. Naor D, Wallach-Dayan SB, Zahalka MA, Sionov RV. Involvement of CD44, a molecule with a thousand faces, in cancer dissemination. Semin Cancer Biol. 2008; 18:260–7. [PubMed: 18467123]
6. Ponta H, Sherman L, Herrlich PA. CD44: from adhesion molecules to signalling regulators. Nat Rev Mol Cell Biol. 2003; 4:33–45. [PubMed: 12511867]
7. Mielgo A, van Driel M, Bloem A, Landmann L, Gunthert U. A novel antiapoptotic mechanism based on interference of Fas signaling by CD44 variant isoforms. Cell Death Differ. 2006; 13:465–77. [PubMed: 16167069]
8. Draffin JE, McFarlane S, Hill A, Johnston PG, Waugh DJ. CD44 potentiates the adherence of metastatic prostate and breast cancer cells to bone marrow endothelial cells. Cancer Res. 2004; 64:5702–11. [PubMed: 15313910]
9. Liu AY, True LD, LaTray L, Ellis WJ, Vessella RL, Lange PH, et al. Analysis and sorting of prostate cancer cell types by flow cytometry. Prostate. 1999; 40:192–9. [PubMed: 10398281]
10. Tsai YS, Lai CL, Lai CH, Chang KH, Wu K, Tseng SF, et al. The role of homeostatic regulation between tumor suppressor DAB2IP and oncogenic Skp2 in prostate cancer growth. Oncotarget. 2014; 5:6425–36. [PubMed: 25115390]

11. Xie D, Gore C, Liu J, Pong RC, Mason R, Hao G, et al. Role of DAB2IP in modulating epithelial-to-mesenchymal transition and prostate cancer metastasis. Proc Natl Acad Sci U S A. 2010; 107:2485–90. [PubMed: 20080667]
12. Yun EJ, Baek ST, Xie D, Tseng SF, Dobin T, Hernandez E, et al. DAB2IP regulates cancer stem cell phenotypes through modulating stem cell factor receptor and ZEB1. Oncogene. 2015; 34:2741–52. [PubMed: 25043300]
13. Marian CO, Yang L, Zou YS, Gore C, Pong RC, Shay JW, et al. Evidence of epithelial to mesenchymal transition associated with increased tumorigenic potential in an immortalized normal prostate epithelial cell line. Prostate. 2011; 71:626–36. [PubMed: 20945502]
14. Weijerman PC, Konig JJ, Wong ST, Niesters HG, Peehl DM. Lipofection-mediated immortalization of human prostatic epithelial cells of normal and malignant origin using human papillomavirus type 18 DNA. Cancer Res. 1994; 54:5579–83. [PubMed: 7923200]
15. Xu D, Lin TH, Li S, Da J, Wen XQ, Ding J, et al. Cryptotanshinone suppresses androgen receptor-mediated growth in androgen dependent and castration resistant prostate cancer cells. Cancer letters. 2012; 316:11–22. [PubMed: 22154085]
16. Lawson DA, Xin L, Lukacs RU, Cheng D, Witte ON. Isolation and functional characterization of murine prostate stem cells. Proc Natl Acad Sci U S A. 2007; 104:181–6. [PubMed: 17185413]
17. Kim M, Turnquist H, Jackson J, Sgagias M, Yan Y, Gong M, et al. The multidrug resistance transporter ABCG2 (breast cancer resistance protein 1) effluxes Hoechst 33342 and is overexpressed in hematopoietic stem cells. Clin Cancer Res. 2002; 8:22–8. [PubMed: 11801536]
18. Zhao L, Wientjes MG, Au JL. Evaluation of combination chemotherapy: integration of nonlinear regression, curve shift, isobologram, and combination index analyses. Clin Cancer Res. 2004; 10:7994–8004. [PubMed: 15585635]
19. Harvey JM, Clark GM, Osborne CK, Allred DC. Estrogen receptor status by immunohistochemistry is superior to the ligand-binding assay for predicting response to adjuvant endocrine therapy in breast cancer. Journal of clinical oncology : official journal of the American Society of Clinical Oncology. 1999; 17:1474–81. [PubMed: 10334533]
20. Kong D, Banerjee S, Ahmad A, Li Y, Wang Z, Sethi S, et al. Epithelial to mesenchymal transition is mechanistically linked with stem cell signatures in prostate cancer cells. PLoS One. 2010; 5:e12445. [PubMed: 20805998]
21. Webber MM, Bello D, Quader S. Immortalized and tumorigenic adult human prostatic epithelial cell lines: characteristics and applications. Part I. Cell markers and immortalized nontumorigenic cell lines. Prostate. 1996; 29:386–94. [PubMed: 8977636]
22. Goodell MA, Brose K, Paradis G, Conner AS, Mulligan RC. Isolation and functional properties of murine hematopoietic stem cells that are replicating in vivo. J Exp Med. 1996; 183:1797–806. [PubMed: 8666936]
23. Pazdur R, Kudelka AP, Kavanagh JJ, Cohen PR, Raber MN. The taxoids: paclitaxel (Taxol) and docetaxel (Taxotere). Cancer treatment reviews. 1993; 19:351–86. [PubMed: 8106152]
24. Abdullah LN, Chow EK. Mechanisms of chemoresistance in cancer stem cells. Clinical and translational medicine. 2013; 2:3. [PubMed: 23369605]
25. Godar S, Ince TA, Bell GW, Feldser D, Donaher JL, Bergh J, et al. Growth-inhibitory and tumor-suppressive functions of p53 depend on its repression of CD44 expression. Cell. 2008; 134:62–73. [PubMed: 18614011]
26. Hwang C. Overcoming docetaxel resistance in prostate cancer: a perspective review. Therapeutic advances in medical oncology. 2012; 4:329–40. [PubMed: 23118808]
27. Carson CC 3rd. Carcinoma of the prostate: overview of the most common malignancy in men. North Carolina medical journal. 2006; 67:122–7. [PubMed: 16752715]
28. Clarke MF, Dick JE, Dirks PB, Eaves CJ, Jamieson CH, Jones DL, et al. Cancer stem cells--perspectives on current status and future directions: AACR Workshop on cancer stem cells. Cancer Res. 2006; 66:9339–44. [PubMed: 16990346]
29. Shaw GL, Wilson P, Cuzick J, Prowse DM, Goldenberg SL, Spry NA, et al. International study into the use of intermittent hormone therapy in the treatment of carcinoma of the prostate: a meta-analysis of 1446 patients. BJU international. 2007; 99:1056–65. [PubMed: 17346277]

30. Dean M, Fojo T, Bates S. Tumour stem cells and drug resistance. Nature reviews Cancer. 2005; 5:275–84. [PubMed: 15803154]
31. Min J, Zaslavsky A, Fedele G, McLaughlin SK, Reczek EE, De Raedt T, et al. An oncogene-tumor suppressor cascade drives metastatic prostate cancer by coordinately activating Ras and nuclear factor-kappaB. Nat Med. 2010; 16:286–94. [PubMed: 20154697]
32. Haegel H, Dierich A, Ceredig R. CD44 in differentiated embryonic stem cells: surface expression and transcripts encoding multiple variants. Developmental immunology. 1994; 3:239–46. [PubMed: 7542511]
33. Patrawala L, Calhoun T, Schneider-Broussard R, Li H, Bhatia B, Tang S, et al. Highly purified CD44+ prostate cancer cells from xenograft human tumors are enriched in tumorigenic and metastatic progenitor cells. Oncogene. 2006; 25:1696–708. [PubMed: 16449977]
34. Zoller M. CD44: can a cancer-initiating cell profit from an abundantly expressed molecule? Nature reviews Cancer. 2011; 11:254–67. [PubMed: 21390059]
35. Screaton GR, Bell MV, Jackson DG, Cornelis FB, Gerth U, Bell JI. Genomic structure of DNA encoding the lymphocyte homing receptor CD44 reveals at least 12 alternatively spliced exons. Proc Natl Acad Sci U S A. 1992; 89:12160–4. [PubMed: 1465456]
36. Legras S, Gunthert U, Stauder R, Curt F, Oliferenko S, Kluin-Nelemans HC, et al. A strong expression of CD44-6v correlates with shorter survival of patients with acute myeloid leukemia. Blood. 1998; 91:3401–13. [PubMed: 9558399]
37. Gunthert U, Hofmann M, Rudy W, Reber S, Zoller M, Haussmann I, et al. A new variant of glycoprotein CD44 confers metastatic potential to rat carcinoma cells. Cell. 1991; 65:13–24. [PubMed: 1707342]
38. Ni J, Cozzi PJ, Hao JL, Beretov J, Chang L, Duan W, et al. CD44 variant 6 is associated with prostate cancer metastasis and chemo-/radioresistance. Prostate. 2014; 74:602–17. [PubMed: 24615685]
39. Kallakury BV, Yang F, Figge J, Smith KE, Kausik SJ, Tacy NJ, et al. Decreased levels of CD44 protein and mRNA in prostate carcinoma. Correlation with tumor grade and ploidy. Cancer. 1996; 78:1461–9. [PubMed: 8839552]
40. Nagabhushan M, Pretlow TG, Guo YJ, Amini SB, Pretlow TP, Sy MS. Altered expression of CD44 in human prostate cancer during progression. American journal of clinical pathology. 1996; 106:647–51. [PubMed: 8929476]
41. De Marzo AM, Bradshaw C, Sauvageot J, Epstein JI, Miller GJ. CD44 and CD44v6 downregulation in clinical prostatic carcinoma: relation to Gleason grade and cytoarchitecture. Prostate. 1998; 34:162–8. [PubMed: 9492843]
42. Maltzman JS, Carman JA, Monroe JG. Role of EGR1 in regulation of stimulus-dependent CD44 transcription in B lymphocytes. Molecular and cellular biology. 1996; 16:2283–94. [PubMed: 8628295]
43. Foster LC, Wiesel P, Huggins GS, Panares R, Chin MT, Pellacani A, et al. Role of activating protein-1 and high mobility group-I(Y) protein in the induction of CD44 gene expression by interleukin-1beta in vascular smooth muscle cells. FASEB journal : official publication of the Federation of American Societies for Experimental Biology. 2000; 14:368–78. [PubMed: 10657993]
44. Anastas JN, Moon RT. WNT signalling pathways as therapeutic targets in cancer. Nature reviews Cancer. 2013; 13:11–26. [PubMed: 23258168]
45. Zeilstra J, Joosten SP, Dokter M, Verwiel E, Spaargaren M, Pals ST. Deletion of the WNT target and cancer stem cell marker CD44 in Apc(Min/+) mice attenuates intestinal tumorigenesis. Cancer Res. 2008; 68:3655–61. [PubMed: 18483247]
46. Clevers H. Wnt/beta-catenin signaling in development and disease. Cell. 2006; 127:469–80. [PubMed: 17081971]
47. Yardy GW, Brewster SF. Wnt signalling and prostate cancer. Prostate Cancer Prostatic Dis. 2005; 8:119–26. [PubMed: 15809669]
48. Lee GT, Kang DI, Ha YS, Jung YS, Chung J, Min K, et al. Prostate cancer bone metastases acquire resistance to androgen deprivation via WNT5A-mediated BMP-6 induction. Br J Cancer. 2014; 110:1634–44. [PubMed: 24518599]

49. Steinbach D, Legrand O. ABC transporters and drug resistance in leukemia: was P-gp nothing but the first head of the Hydra? Leukemia : official journal of the Leukemia Society of America, Leukemia Research Fund, UK. 2007; 21:1172–6.

50. Zardavas D, Baselga J, Piccart M. Emerging targeted agents in metastatic breast cancer. Nature reviews Clinical oncology. 2013; 10:191–210.

Transitional relevance

Castration resistant prostate cancer (CRPC) recognized as a lethal disease has been implied to derive from stem cell population associated with its resistance to anti-androgen therapy and chemotherapy. In this study, we demonstrate that immortalized normal human prostate epithelial cells, appeared non-tumorigenic in vivo, become tumorigenic, androgen-independent, and acquire stem cell phenotypes with chemo-resistance after knocking down a novel tumor suppressor gene (i.e., DAB2IP). The clinical data also indicate an inverse correlation between the expression of DAB2IP and stem cell biomarker during prostate cancer progression. We further unveil that the Wnt pathway is a key underlying mechanism that leads to CSC. Thus, by targeting CSCs using Wnt small molecular inhibitors synergistically enhance the efficacy of conventional chemotherapy both *in vitro* and *in vivo* models. This study offers a new promising therapeutic strategy targeting CSC in CRPC therapy.

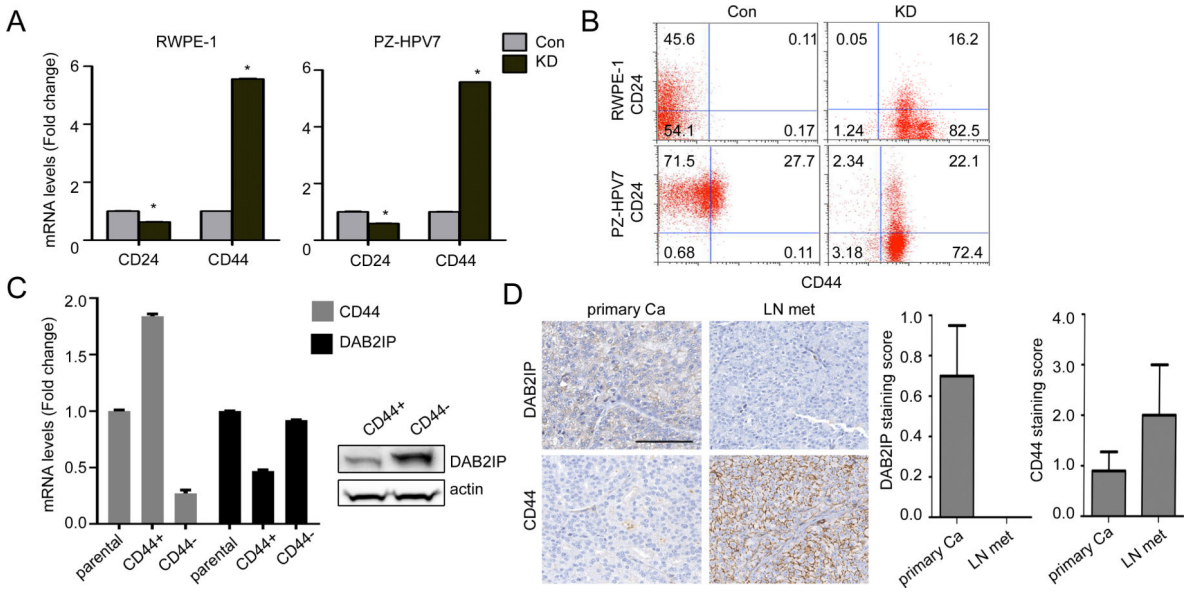

Figure 1. Stem-like CD44^{+}/CD24^{-} cell population are increased in KD cells

(A) Expression levels of CD24 and CD44 mRNA were analyzed by qRT-PCR. After normalizing with 18S rRNA in each sample, the relative mRNA levels were calculated using control (=1). *, p<0.01. (B) Cells were co-stained with APC conjugated CD24 and PE conjugated CD44 and analyzed by flow cytometry. APC-IgG and PE-IgG were used as the negative control for gating and the labels indicated the percentage of each cell population. (C) CD44 and DAB2IP mRNA (left panel) and protein (right panel) expressions were compared in CD44^{+} and CD44^{-} population sorted from PZ-HPV7T cells. (D) Representative IHC staining of DAB2IP and CD44 in clinical specimens (left panel). The scale bar represents 100 μm. Right panel: DAB2IP and CD44 staining score in primary PCa were compared with the metastatic tissue.

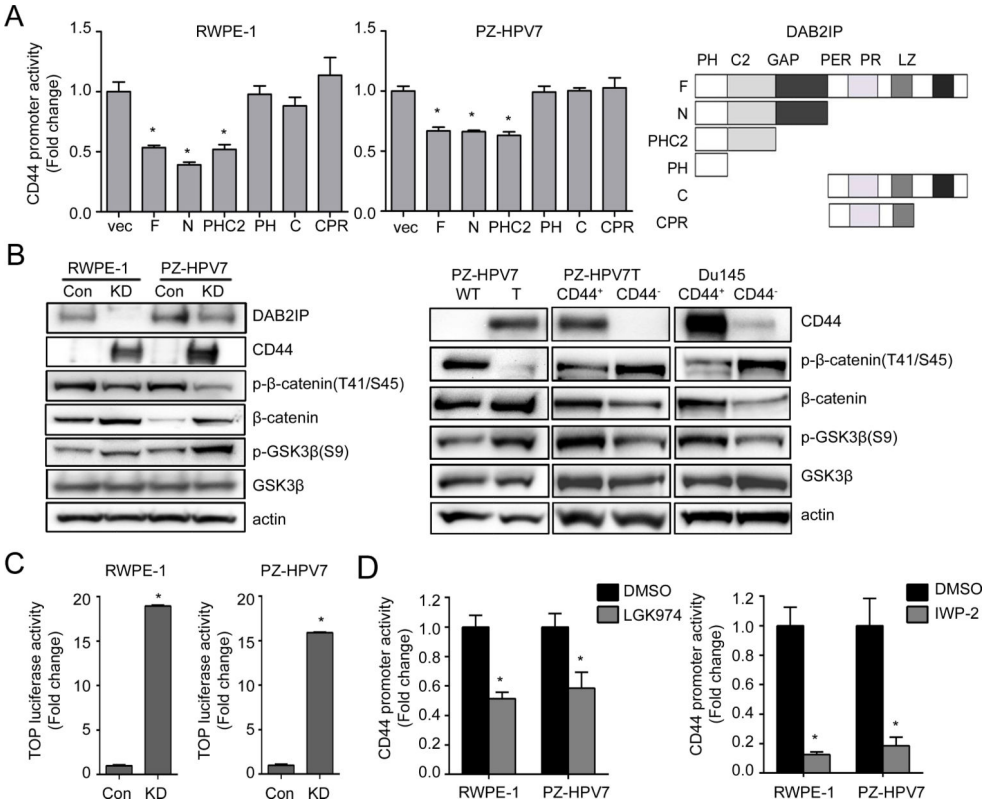

Figure 2. C2 domain of DAB2IP is the key domain for suppressing CD44 expression

(A) RWPE-1 and PZ-HPV7 KD cells were co-transfected with various DAB2IP domains and CD44-luc plasmid, and then luciferase activity was determined. Asterisk indicates statistical significance in cells transfected with vector versus F, N, and PHC2 domain (*P<0.01*). (B) Wnt pathway related genes expressions were compared in RWPE-1 and PZ-HPV7 Con and KD subline (left panel), and PZ-HPV7 WT and T, or CD44+ and CD44- population sorted from Du145 and PZ-HPV7T cells (right panel), respectively. (C) Cells were transfected with TOP for 48 h and subjected to dual luciferase assay. (D) RWPE-1 KD or PZ-HPV7 KD cells were transfected with CD44-luc plasmid for 24 h and treated with 200 nM LGK974 (left panel) or 5 μM IWP-2 (right panel) for another 24 h, then subjected to dual luciferase assay.

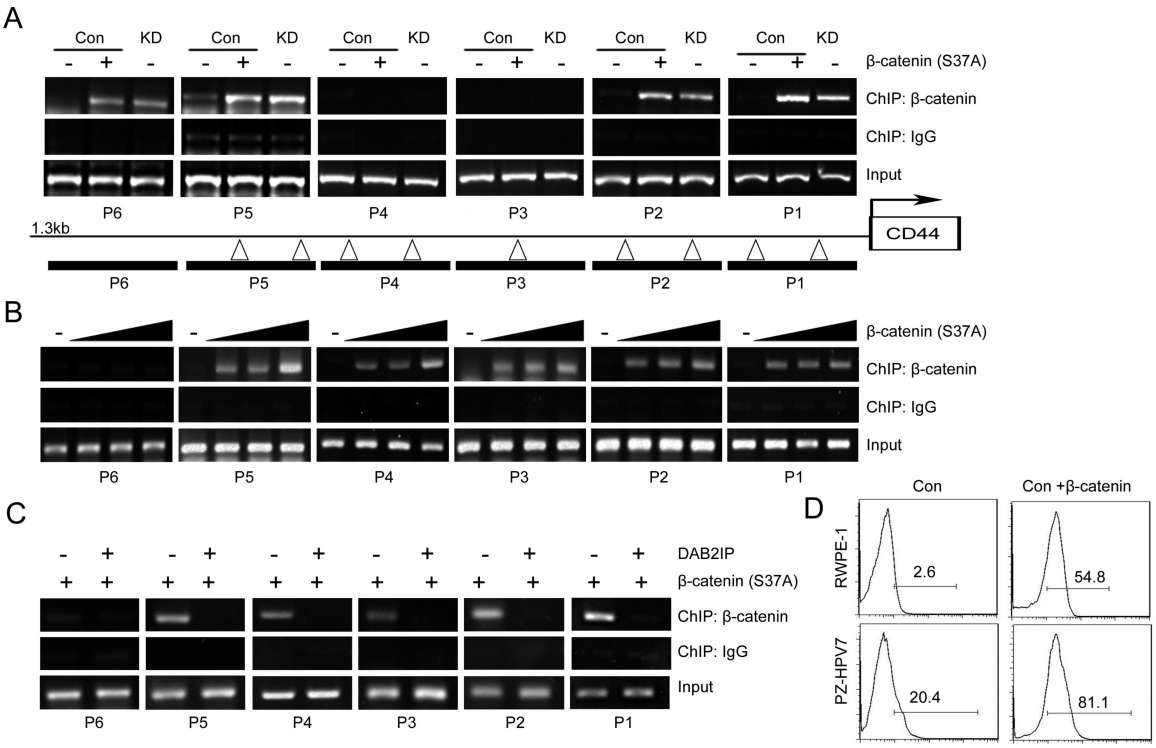

Figure 3. Characterization of the binding of β-catenin to CD44 promoter region

(A) β-catenin binding to the CD44 promoter region was evaluated by ChIP assay. Chromatin DNAs prepared from PZ-HPV7 Con and KD cells were immunoprecipitated with β-catenin antibody and subjected to PCR. (Δ) in CD44 promoter regions. (B) β-catenin plasmid was transfected to 293 cells for 48 h and direct binding of β-catenin to the CD44 promoter was evaluated by ChIP. Rabbit IgG (immunoglobulin G) was used as the negative control. (C) DAB2IP and β-catenin plasmid were co-transfected to 293 cell and ChIP assay was performed after 48 h. (D) Con cells from RWPE-1 or PZ-HPV7 were transfected with CA β-catenin mutant (S37A) for 48 h and the expression levels of CD44 were compared using flow cytometry.

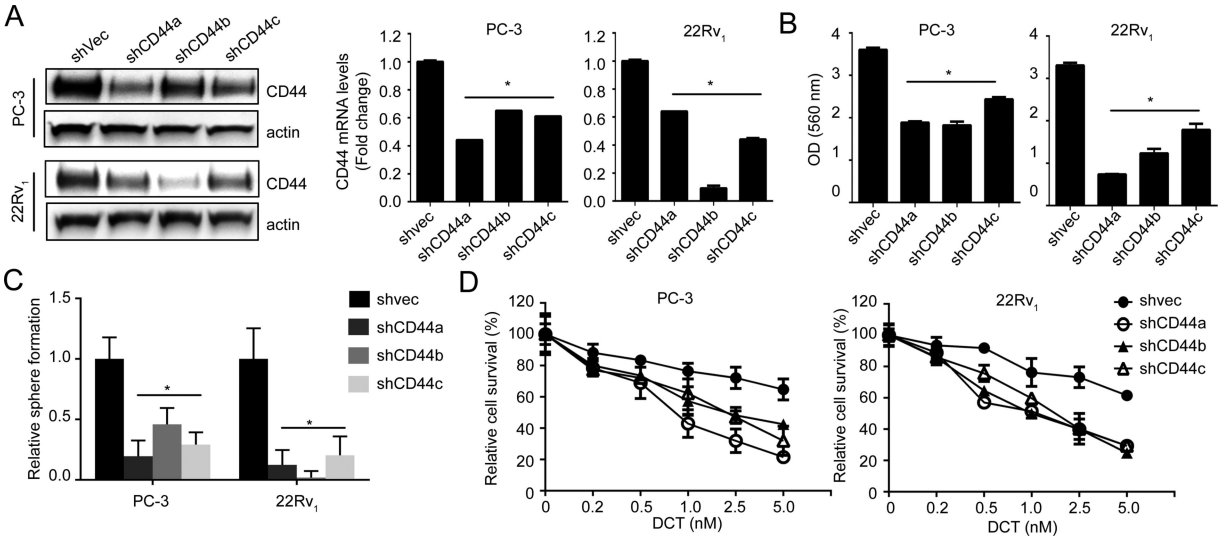

Figure 4. CD44 is critical for PCSC development and its chemo-resistance

(A) Characterization of shCD44 sublines of PC-3 and 22Rv1 cells generated using shRNA (Origene, TG314080) transfection by qRT-PCR and Western blot analyses. (B) Clonogenic assay of shCD44 or shvec cells were seeded in 6-well plates at a density of 500 cells per well and cultured for 10 days then stained with Crystal violet. The relative number of colony was determined by measuring $OD_{560\ nm}$. (C) Prostaspheres assay was performed for 2 weeks and the numbers of prostaspheres were compared in shvec and shCD44 cells. (D) Cells were seeded in a 96-well and treated with docetaxel for 48 h. Cell viability was assessed by MTT assay.

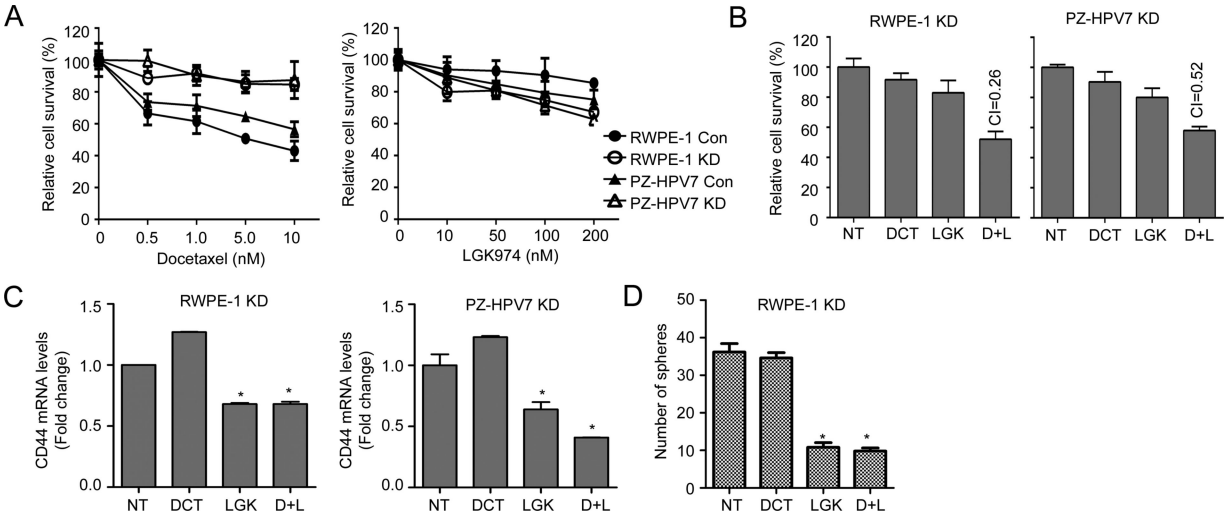

Figure 5. Wnt inhibitor reduces chemoresistance of KD cells to docetaxel

(A) Cells were treated with docetaxel or LGK974 for 48 h and subjected to MTT assay. (B) Cells were treated with 1 nM Docetaxel, 100 nM LGK974, or combination. And cell viability was determined 48 h after treatment by MTT assay and drug synergistic effects were determined based on combination index (CI). CI<1, synergistic; CI=1, additive; CI>1, antagonistic effect. NT, Non-treatment; DCT, docetaxel; LGK, LGK974; D+I, docetaxel and LGK974 combination treatment. (C) The expression levels of CD44 mRNA were analyzed 48 h after treatment by qRT-PCR. (D) The prostasphere formation was determined from cells after 24 h treatment then plated into sphere culture condition for 2 weeks. Media containing each drug were changed every 3 days.

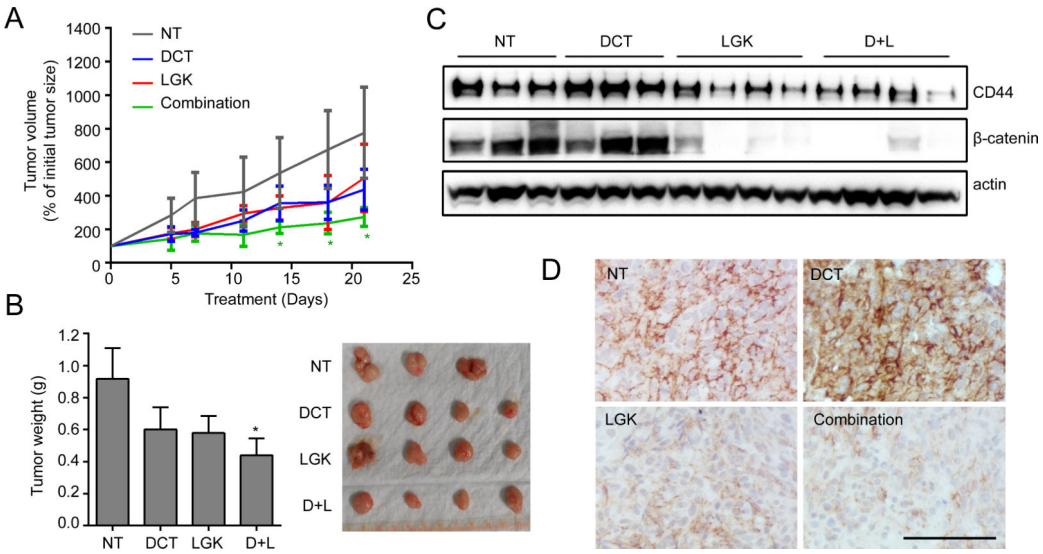

Figure 6. Combination therapy targeting CD44^{+} population sensitizes Du145 xenograft to conventional therapy

(A) Du145 cells were subcutaneously injected into SCID mice and treatment started when tumors became palpable (> 100 mm^3). The mice were treated with docetaxel (5 mg/kg/i.p.), LGK974 (2 mg/kg/oral gavage), or combination twice a week for 3 weeks. (B) After 3 weeks treatment, xenograft tumors were excised and photographed. (C) The expression levels of CD44 and β-catenin in xenograft tumors were analyzed by Western blot analysis. (D) Representative IHC results of CD44 in xenograft tumors after treatment were displayed. Scale bar, 100 μm.